

## Preparation, characterization and evaluation of metformin encapsulated in PEGylated magnetic Niosome: For molecular targeted therapy of lung cancer

Rasoul shahbazi<sup>a</sup>, Zohreh Mirjafary<sup>a\*</sup>, Nosratollah Zarghami<sup>b\*</sup>, Hamid Saeidian<sup>c</sup>

<sup>a</sup> Department of Chemistry, Science and Research Branch, Islamic Azad University, Tehran, Iran

<sup>b</sup> Department of Medical Biochemistry, Faculty of Medicine, Istanbul Aydin University, Turkey

<sup>c</sup> Department of Science, Payame Noor University (PNU), P.O.Box 19395-3697, Tehran, Iran

Received: February 2024; Revised: February 2024; Accepted: March 2024

**Abstract:** It was proven that metformin (MET), a phytochemical broadly used drug in the treatment of type 2 diabetes and Polycystic ovary syndrome (PCOS), can prevent the growth and reproduction of various human tumors like lung cancer cells. Also, in past studies, it was found that MET shows an excellent anti-cancer effect by diminishing the proliferation and stimulating the apoptosis of various cancerous cells. In this study, in the first stage, we synthesized the PEGylated (polyethylene glycol) magnetic niosome (MNio) nanoparticles (NPs) loaded by MET, in the next stage, we evaluated the reaction of MET on the invasion abilities and migration of the A549 cancer cell line in the *in vitro* condition to create a novel and targeted drug delivery system. Cytotoxicity assay showed that the growth of A549 cell lines was barricaded by free and PEGylate magnetic niosomal metformin (PEG-M-Nio-MET). It was proven that encapsulation of MET in modified niosome decreases the amount of IC<sub>50</sub> in the A549 cell line. Also, RT-PCR results demonstrated that the expression levels of the BCL-2 and BAX were considerably decreased in the A549 cancer cell line with PEG-M-Nio-MET and Nio-MET compared to free MET. It is predicted that the application of encapsulated MET in the modified magnetic niosome could significantly improve the treatment efficiency of human lung cancer.

**Keywords:** Lung cancer, Metformin, Targeted drug delivery system, Magnetic Niosome

### Introduction

Lung cancer is one of the most common cancers all over the world. Abnormal cells start to grow and spread throughout the lung uncontrollably. Lung cancer causes critical health problems that lead to the death of the patient. Some common symptoms of lung cancer disease are shortness of breath, chest pain, haemoptysis (coughing up blood), persistent cough and lung infections [1, 2]. Small cell carcinoma (SCLC) and [3] are the most prevalent kinds of lung cancer, SCLC is less prevalent but growth rapidly, while NSCLC is the most prevalent but growth sluggishly.

Some diagnostic techniques for lung cancer are MRI (magnetic resonance imaging), chest X-rays, biopsy and bronchoscopy. Therapy of lung cancer is dependent on the extent of expansion and the kind of cancer. Early and timely diagnosis of cancer may cause acceptable results and effective treatment. Some effective treatments for lung cancer include radiotherapy (radiation), surgery and chemotherapy commonly used based on the stage and type of cancer. In the chemotherapy technique, drugs target quickly dividing cancer cells and also some normal cells. Despite the cancer drugs are more efficient, they show considerable side effect that leads to a reduction in the dose of chemotherapy drugs [4]. These side effects are

Corresponding author: Email: Zmirjafary@srbiau.ac.ir

overcome by utilizing novel drug delivery systems like niosome (Nio), liposome (Lip), polymer and micelle. Nio is a novel nano vesicle utilized in novel drug delivery systems. Nios are prepared with cholesterol (Chol) and non-ionic surfactants to create a bilayer vesicle [5-8]. Nios superiority over other nano-carriers is that they can encapsulate both hydrophilic and hydrophobic anti-cancer drugs in the lipid bilayer and aqueous layer. Nios enhances the half-life of both drugs in the cancerous cells. The non-ionic surfactant used in Nios structure is biocompatible and biodegradable, therefore, it is compatible with the human immune system [9, 10]. Chol increases the stability and decreases the leakage of Nio, causing to improvement in the entrapment efficiency (EE) of the entrapped drugs [11]. Recently, novel magnetic niosome (MNio) loaded with anticancer phytochemical drugs have been evaluated [12]. Hopeful outcomes are reports about various drugs released at the cancerous tissue by applying an external magnetic field (EMF). MNio has a major and necessary role in biomedicine, especially in the area of novel drug delivery systems. In this study pay special attention to Nio-PEG-MNPs-MET due to their magnetic properties in the exact targeting of the MET entrapped in PEGylated magnetic niosome into the desired cancerous tissue [13, 14]. The amalgamation of MNPs and Nio enables both drug protection attributes and well as drug-targeting, this makes Nio-PEG-MNPs-MET an effective nano-carrier for novel and efficient drug delivery systems. It is possible to synthesize the Nio-PEG-MNPs-MET by enclosing MNPs and MET inside the Nios. Phytochemical drugs are generally the extract of pharmaceutical plants with various remedial utilizations. In the past several decades, scholars have attention to plant extracts, due to their anti-neoplastic and anti-cancer attributes [15]. Metformin is an extract isolated from the pharmaceutical plant *Galega officinalis*. MET has the major active group of guanidine (nitrogen-rich organic compound) in structure that barricade the growth of cancerous cells and reduce the possibility of expansion solid tumors, including breast, colon and ovarian cancers [2, 16-20]. Previously, MET was used as type 2 antidiabetic agent, which adjust glucose homeostasis by restriction of liver glucose preparation and enhancement in muscle glucose uptake [21, 22]. Nowadays, the anticancer feature of MET is

identify to be relevant to the attendance of guanidine groups to inhibit cancer cells, interaction with DNA, invasion and participate with the cell cycle [23]. MET has some side effects like allergic reactions, chest pain, gastric discomfort, high dose (2–3 times a day) and lactic acidosis [24, 25]. Hence, novel drug Nano-carrier for Met are necessary to overcome mentioned side effects causes to systemic drug dispensation and attain most therapeutic effect [26, 27]. This study performed to evaluate the role of MET encapsulated in Nio-PEG-MNPs in compare with free MET in targeting the A549 lung cancer cell line. For this purpose, Nio-PEG-MNPs-MET was prepared by TFH method and their morphological and physio-chemical properties were investigated [13, 28, 29]. In the following, the MTT assay was used to evaluate cell viability. In addition, apoptosis, cellular uptake rate and cell cytotoxicity effects of Nio-PEG-MNPs-MET were evaluated *in vitro* [30, 31] (Scheme 1).

## Experimental

### Materials and Methods

#### Materials

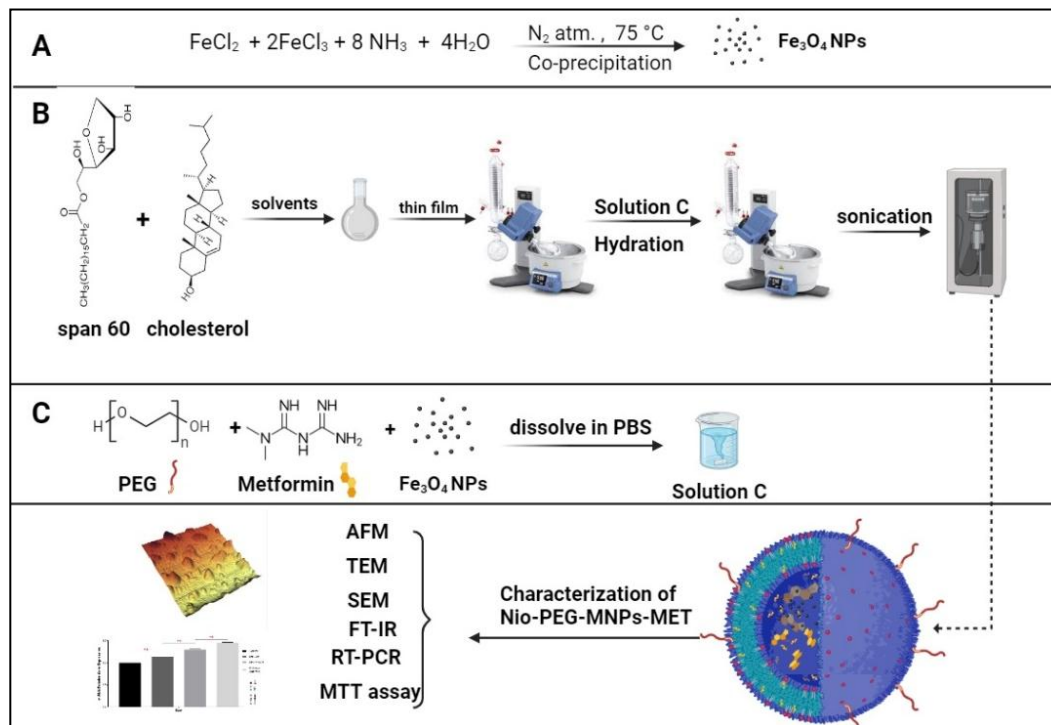
Metformin hydrochloride, Sorbitan monostearate (Span 60), cholesterol, DMEM (Dulbecco's Modified Eagle Medium), Dialysis tubing (cellulose membrane avg. flat width 1 cm and molecular weight cut-off 14000 Da), dimethyl sulfoxide (DMSO), 3-(4, 5 dimethylthiazol-2-yl)-2, 5-diphenyltetrazolium bromide (MTT), trypsin, phosphate-buffered saline (PBS), Iron (III) chloride hexahydrate ( $\text{FeCl}_3 \cdot 6\text{H}_2\text{O}$ ), Iron (II) chloride tetrahydrate ( $\text{FeCl}_2 \cdot 4\text{H}_2\text{O}$ ), polyethylene glycol (PEG, MW 4000), methanol and chloroform were obtained from Sigma-Aldrich (St Louis, MO). A549 cells were obtained from the Tabriz University of Medical Sciences (Faculty of Advanced Medical Sciences).

#### Synthesis of magnetic nanoparticles

Commonly, the co-precipitation technique was performed to prepare magnetic nanoparticles (MNPs) (Scheme 1A). briefly,  $\text{FeCl}_3 \cdot 6\text{H}_2\text{O}$  (5.50 g, 2 mol) and  $\text{FeCl}_2 \cdot 4\text{H}_2\text{O}$  (4 g, 1 mol) was dissolved in 60 mL of deionized water in a flask and under  $\text{N}_2$  atm (atmosphere) with strong stirring at 75 °C for 2 hours. Ammonium hydroxide ( $\text{NH}_4\text{OH}$ , 15 mL) was inserted into the mixture drop-wise,

stirred under  $N_2$  atm for another 2 hours, then placed at room temperature to cool. The  $Fe_3O_4$  NPs as black sediments were deposited on the bottom of the flask. Black sediments were collected by an external magnet and washed several times with deionized water and ethanol until neutral pH to

eliminate impurities. Finally, the black powder was dried at  $75\text{ }^\circ\text{C}$  for 24 hours to prepare the final pure products [32].



**Scheme 1.** Synthesis of Nio-PEG-MNPs-MET with thin-film hydration method. Nio: niosome, PEG: Polyethylene glycol, MNPs: magnetic nanoparticles, MET: metformin

### Synthesis of NIOs by thin film hydration method

The Nio vesicles were synthesized by the thin film hydration (TFH) technique (Scheme 1B) [28, 33]. Generally, 36 mg of Span 60 and 5 mg of cholesterol were dissolved in 6 mL of methanol and 3 mL of chloroform solvents (with a 2:1 ratio) in a special rotary evaporator round bottom flask (containing Glass beads). The prepared solutions solvents were evaporated by a rotary evaporator device to form a thin dry film ( $60\text{ }^\circ\text{C}$ , 120 rpm, 60 min). MET (3 mg), PEG (3 mg) and MNPs (1.5

mg) were dissolved in PBS (PH 7.4) then the thin dry film was hydrated by this solution (120 rpm, 60 min) for the formation of Nio-PEG-MNPs-MET (Scheme 1C) [19, 33, 34]. Then the milky-like mixture was collected into a Falcon 15 ml and kept at  $4\text{ }^\circ\text{C}$  for prevention of agglomeration. The milky-like mixture was sonicated by using a probe sonicator (bandelin, sonopuls, Berlin, Germany) at  $4\text{ }^\circ\text{C}$  for 15 min [30, 35]. The prepared samples were kept in the refrigerator for later evaluation. The structure of the evaluated Nio formulations is shown in Table 1.

**Table 1.** Composition of various niosomal formulations (molar ratio)

Formulation	independent variables (molar ratio)				Dependent Variables		
	Span60	Cho	PEG	MNPs	PDI	Nio size (nm)	EE%

Nio-MET	1	1	0	0	0.345	280	72
Nio-MET	3	1	0	0	0.312	265	75
Nio-MET	5	1	0	0	0.290	275	77
Nio-MET	8	1	0	0	0.190	215	85
Nio-PEG-MET	5	1	1	0	0.215	285	82
Nio-PEG-MET	8	1	1	0	0.205	240	88
PEG-Nio-MNPs-MET	5	1	1	1	0.202	280	83
PEG-Nio-MNPs-MET	8	1	1	1	0.195	235	89

Nio: niosome, MET: metformin, PEG: Polyethylene Glycol, MNPs: magnetic nanoparticles, Cho: cholesterol, PDI: Polydispersity Index, EE: Encapsulation Efficiency.

### Characterizations of Niosomal Formulation

The Nio size, zeta potential and polydispersity index (PDI) were investigated by a zeta sizer instrument (Malvern, UK) at 25 °C. various Nio morphology was evaluated by transmission electron microscopy (TEM). In such a way that a few drops of Nio were poured on a carbon film-coated copper grid and sample morphology was characterized by TEM at 100 kV (LEO906E, Carl Zeiss, Oberkochen, Germany). A Field Emission Scanning Electron Microscope (FE-SEM) (Seron Technologies, Gyeonggi-do, Korea) was used to evaluate the morphology of the synthesized Nio. First, put some drops of a diluted best Nio formulation (1:1000) on the SEM holder. Covered it with a layer of gold, and put the SEM holder in the device (2 atm, 3 min). Atomic Force Microscopy (AFM) (AFM, Brisk, Frankfurt Germany) was utilized to analyze the size and morphologies of the Nios. A diluted sample (1:1000) was dropped on the AFM mica holder and dried at room temperature then evaluated by the device. The FT-IR spectra of Span 60, Chol, MET, blank Nio, Nio-PEG-MNPs-MET, PEG and MNPs were evaluated in a range of 400 to 4000  $\text{cm}^{-1}$  (PerkinElmer FT-IR, USA).

### Fourier-Transform Infrared Spectroscopy (FT-IR)

The molecular interactions of MET, span60, cholesterol, blank Nio, Nio-PEG-MNPs-MET and PEG were investigated by FT-IR (Bruker Tensor 27 FT-IR Spectrometer, Canada). For this test, all samples were separately investigated in KBr discs and their assay was utilized in the range of 4000 to 400  $\text{cm}^{-1}$  at room temperature.

### Assessment of encapsulation efficiency (EE)

The EE% of various Nio was investigated indirectly by calculating free MET after centrifugation by an Amicon (Ultra 15 membrane) at 4 °C at 4000 rpm for 25 min. The free MET was removed *via* the membrane and the MET-loaded Nio was stuck in the upper chamber. In the following, the concentration of free MET was evaluated at 232 nm wavelength by a UV-Vis spectrophotometer. The amount of EE was measured by the following equation:

Entrapment efficiency (EE) % =  $[(C_i - C_f) / C_i] \times 100$   
 $C_i$  is the primary MET concentration for Nio synthesis and  $C_f$  is the concentration of free MET after centrifugation.

### Assessment of drug release

A solution (2 mL) of Nio-PEG-MNPs-MET and Nio-MET were inserted in the dialysis bag (cellulose membrane average flat width 10 mm and

molecular weight cut-off 14000 Da). Then plunged in 50 mL release solution (SDS-PBS 0.5 % w/v) with gradual stirring (60 rpm) for 72 h at 37 °C in various PH (1.2, 5.4 and 7.4). At the determined period (1, 6, 12, 24, 48 and 72 h), 1 mL of release solution was taken and replaced with fresh solution. The amounts of releases were evaluated at 232 nm by UV-vis spectroscopy (for every sample). Considering that the free MET is the control.

### MTT assay

The MTT assays are one of the first methods to investigate the cytotoxicity of nanocarriers and drugs on cell proliferation. The MTT assay was used to evaluate the cytotoxicity and synergistic inhibitory of free MET, modified niosome-loaded-MET and their combination after 48 h drug therapy. The A549 cancer cell lines were seeded at a density of  $5 \times 10^5$  cells/well in RPMI additives with 10% FBS and 1x penicillin-streptomycin. After 48 h incubation, the cells were remedied with various concentrations of MET, Nio-MET and Nio-PEG-MNPs-MET (free MET con. 0, 5, 10, 15, 30 and 40 mM), (Nio MET concentration 0, 25, 50, 100, 150 and 200  $\mu$ M). After 48 h, 5 mg/mL MTT was inserted into every cell culture well and the plates were coated with a thin layer of aluminum and incubated for 4 h at 37°C under 5% CO<sub>2</sub>. The viability rate of cells was investigated by utilizing an ELISA microplate reader (BioTek Power Wave XS) and the absorbance rate at 570 nm was calculated and a reference wavelength of 630 nm. The percentage of the Cell viability was calculated by utilizing the formula shown below:

$$\text{percentage of cell viability (\%)} = \frac{OD_t}{OD_c} \times 100$$

Where OD<sub>t</sub> is the OD<sub>630-570</sub> treatment and OD<sub>c</sub> is the OD<sub>630-570</sub> control (optical density).

### Gene Expression Analysis

An RT-PCR assay was utilized to evaluate the transcription mRNA of BCL-2 and BAX genes. In the first stage,  $1.2 \times 10^6$  A549 cancer cells were seeded in 6-well plates and incubated with 5% CO<sub>2</sub> at 37 °C for 24 h. then, cells were treated with free MET, Nio-MET and Nio-PEG-MNPs-MET at their determined IC<sub>50</sub> concentration. After 48 hours of treatment of free MET, Nio-MET and Nio-PEG-MNPs-MET, all mRNAs were extracted by Trizol

reagent (Merck, Germany) according to protocol. After that, by calculating the OD<sub>260</sub>/OD<sub>280</sub>, the quality and amounts of all extracted mRNAs were investigated. In the next stage, utilizing a cDNA synthesis kit (Fermentas, Vilnius, Lithuania), cDNAs were prepared from mRNA extracted from every sample following the producer's protocol.

### Statistical analysis

Statistical analysis was accomplished by Graph Pad Prism software (version 10, Boston, USA). Two-way and One-way analysis of variance (ANOVA) was utilized to calculate the importance level of the diversity between groups (p-value < 0.05). All information was presented as mean  $\pm$  SD from 3 independent experiments.

## Results and discussion

### Characterization of synthesized Nio-PEG-MNPs-MET

The morphology and size of various modified Nios were evaluated by dynamic light scattering (DLS), transmission electron microscopy (TEM), Atomic Force Microscopy (AFM) and Field Emission Scanning Electron Microscope (FE-SEM). The size of Nio calculated by DLS was bigger than that observed on SEM images (Figure 2B). This distinctness between the two tests may refer to the drying of Nios prepared for the SEM test. According to the SEM picture (Figure 1B), synthesized Nios has a semi-uniform spherical shape. The SEM picture proved that the Nios have spherical morphology. Generally, the SEM picture demonstrates the morphological data of dried Nio, while DLS calculates the hydrodynamic size that involves the size of adsorbed molecules on the Nio surface and core. The TEM picture (Figure 1A) demonstrated that the synthesized Nio has a spherical structure. In addition, the zeta potential of Nio-PEG-MNPs-MET and Nio-MET were calculated -15 mV and -32.4 mV, respectively (Figure 2A). Based on the results of AFM (Figure 1C), which are completely in agreement with DLS results and SEM pictures and show the size and particle structure with a height of 69 nm from the surface. Like as SEM pictures, the size of Nio was smaller than the results calculated by the DLS technique due to the dehydration of Nios [36-39]

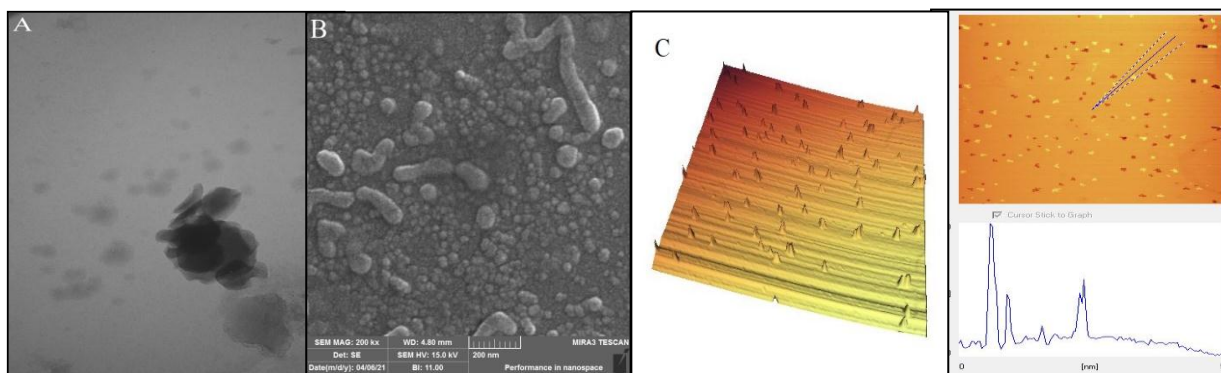


**Figure 1.** Morphological assay of Nio-PEG-MNPs-MET. (A) transmission electron microscopy (TEM), (B) scanning electron microscopy (SEM), (C) Atomic Force Microscopy (AFM); Nio: niosome, PEG: Polyethylene Glycol, MNPs: magnetic nanoparticles, MET: metformin.

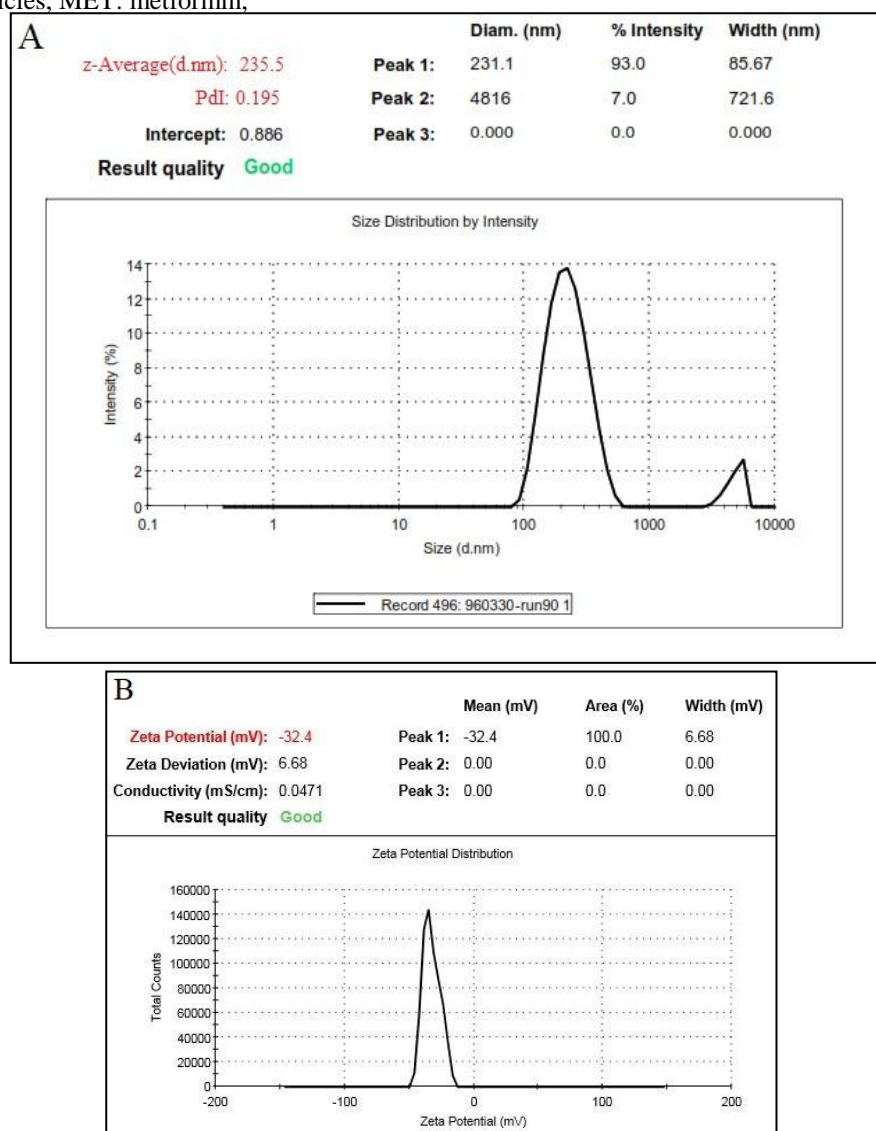


**Figure 2.** (A) Size and PDI, (B) zeta potential of Nio-PEG-MNPs-MET; PDI: polydispersity index, Nio: niosome, PEG: Polyethylene Glycol, MNPs: magnetic nanoparticles, MET: metformin.

### FT-IR Spectroscopy Analysis

Fourier-transform infrared spectroscopy (FT-IR) was evaluated to prove the existence of MET in various Nio formulations for targeted drug delivery. The FT-IR spectrum of pure metformin Hydrochloride in Figure 3c shows some specific sharp and broad peaks that include 1200-950  $\text{cm}^{-1}$  (C-N stretching), 1600-600  $\text{cm}^{-1}$  (N-H deformation), 3020-2850  $\text{cm}^{-1}$  ( $(\text{CH}_3)_2\text{N}$  absorption) and 3370  $\text{cm}^{-1}$  (N-H stretching). The FT-IR pattern for empty Nio (Figure 3d) displays some specific peaks in the range of 3450–1120  $\text{cm}^{-1}$ . The C-H stretching was in the region of 2850–3000  $\text{cm}^{-1}$  refer to Span 60 and cholesterol. The broad peak at 3450  $\text{cm}^{-1}$  was O-H stretching of Span 60 and cholesterol. the FTIR spectrum of cholesterol shows several peaks, where the O-H stretching at 3450  $\text{cm}^{-1}$ , C-H stretching in the region of 2750–3000  $\text{cm}^{-1}$ , C=C stretching at 1675  $\text{cm}^{-1}$ , C-C stretching at 1506  $\text{cm}^{-1}$  and  $\text{CH}_2$  deformation and  $\text{CH}_2$  bending in the region of

1030–1400  $\text{cm}^{-1}$  (Figure 3a). The FT-IR spectrum of Span 60 demonstrates some specific peaks including C–O stretching at 1120  $\text{cm}^{-1}$ , the C–H stretching in the region of 2850–3010  $\text{cm}^{-1}$  and O–H stretching at 3450  $\text{cm}^{-1}$  (Figure 3b). In addition, the FT-IR spectrum captured from Nio-PEG-MNPs-MET demonstrated a small peak that was referred to as the  $\text{CH}_2$  chain of PEG, proving the existence of PEG in the Nio structure at 1360  $\text{cm}^{-1}$  (Figure 3f). For pure PEG, the broad peaks appear at 3445  $\text{cm}^{-1}$  (O-H stretching), 2869  $\text{cm}^{-1}$  (C-H stretching), 1453  $\text{cm}^{-1}$  (C-H bending vibrations from  $\text{CH}_2$  groups), 1245  $\text{cm}^{-1}$  (C-O stretching vibration) and the peak observed at 1075  $\text{cm}^{-1}$  refer to C-O-C symmetrical stretching (Figure 3g). The FT-IR spectrum of  $\text{Fe}_3\text{O}_4$  NPs shows some peaks at 585 and 635  $\text{cm}^{-1}$  that are related to Fe-O stretching-vibration, O-H stretching at 3430  $\text{cm}^{-1}$  and some peaks at 1385, 1630, 2865 and 2930  $\text{cm}^{-1}$  are related to O-H bending due to de-ionized water used as solvent (Figure 3h).

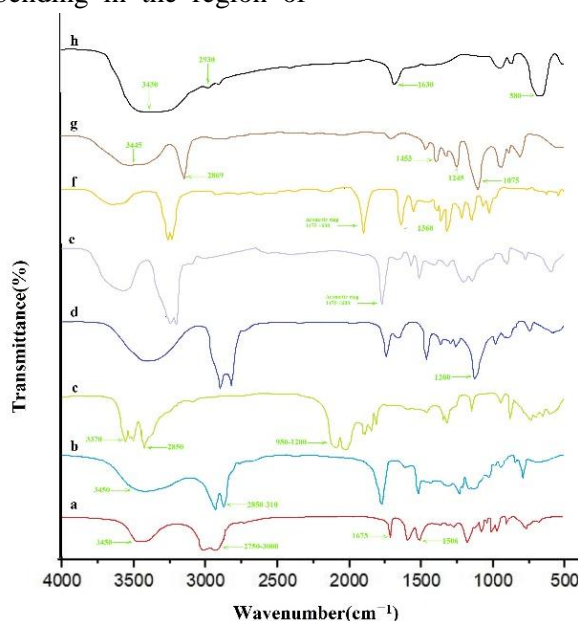


**Figure 3.** FT-IR Spectra of (a) cholesterol, (b) Span 60, (c) MET, (d) blank Nio, (e) Nio-MET, (f) Nio-PEG-MNPs-MET, (g) PEG, (h)  $\text{Fe}_3\text{O}_4$ ; MET: metformin, Nio: niosome, PEG: Polyethylene Glycol, MNPs: magnetic nanoparticles.

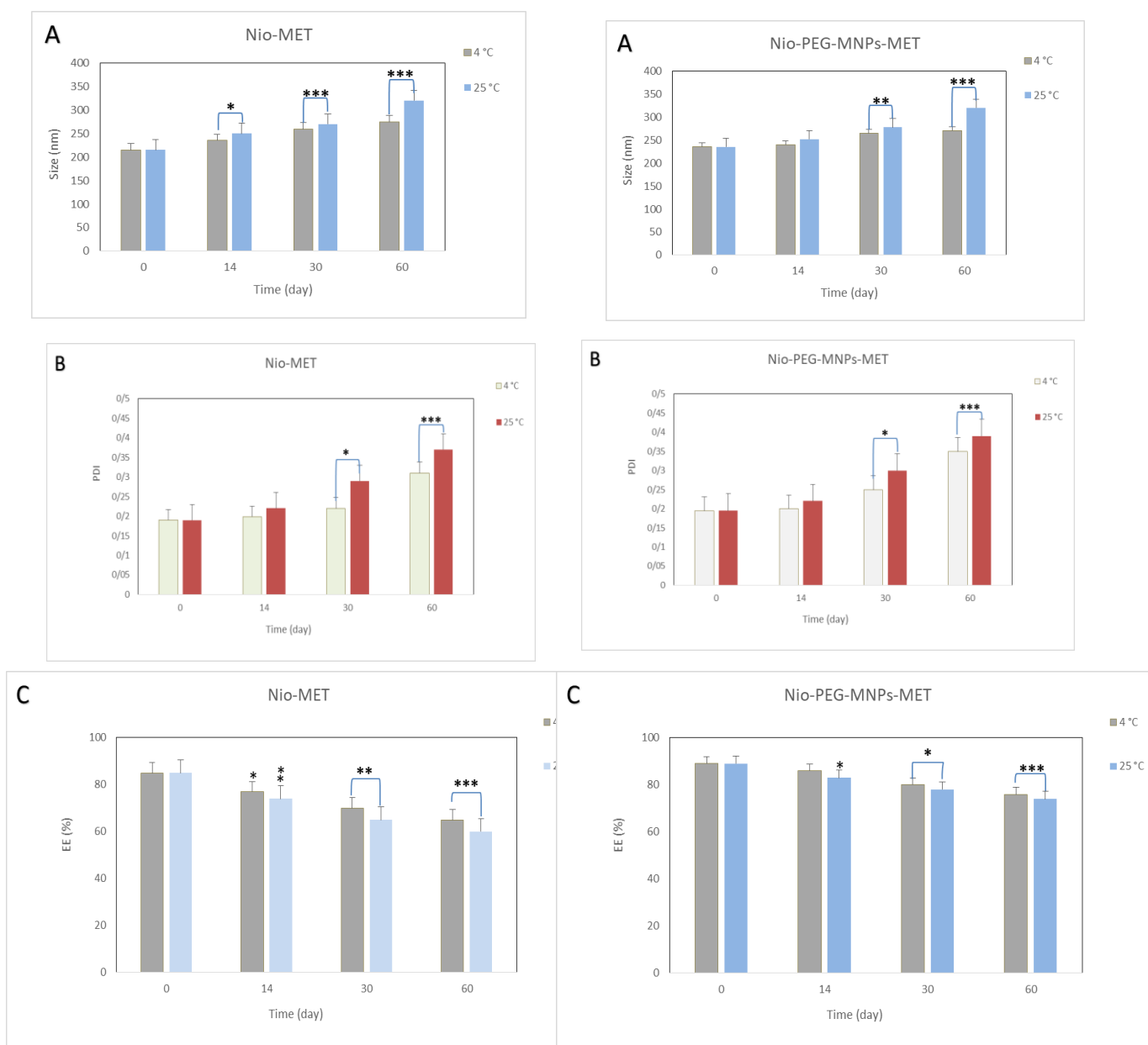
### Physical Stability of Nio-PEG-MNPs-MET

An optimal and stable Nio has a uniform nanoparticle size and a high ability to encapsulate drugs without any leakage. Therefore, the PDI, Nio size and rate of MET remaining in the Nio-MET and PEG-MNPs-Nio-MET formulations were evaluated for 2 months in two storage conditions

( $25 \pm 2$  °C and  $4 \pm 2$  °C) (Figure 4). The evaluation of the empirical data (Figure 4) proved that the PDI, entrapment efficiency and particle size of the Nio-PEG-MNPs-MET formulation stored in both conditions have more efficient stability than the other formulations. A notable difference was shown between the Nio-PEG-MNPs-MET and Nio-MET formulations stored at 25 °C and 4 °C in

terms of EE%, PDI and particle size. According to the results obtained, the attendance of PEG in the Nio structure showed more efficient effects on the EE%, PDI and particle size after 2 months of storage. This demonstrated that the PEGylation of Nios may eliminate the problems related to Nio instability including drug leakage, aggregation and fusion. Regardless of the physical stability of Nio-PEG-MNPs-MET and Nio-MET drug delivery systems during the storage time, it was demonstrated that the encapsulated drug leaked gently from various Nios, chiefly at 25 °C (room temperature). According to the results of the storage in two different conditions, there is a

straight relation between the EE% and storage period (Figure 4C). Also, the enhancement of temperature is a reason for increasing the rate of Nio leakage. In addition, because of the aggregation and fusion of Nios, the PDI and average particle size may increase in storage time (Figure 4A and B). This increase was bigger at 25 °C than the 4 °C. These cases may be related to as slow mobility and permeability of Nio at 4 °C temperature, while Nio stored at room temperature tends to stick together and create bigger Nios. According to the results, the Nio-PEG-MNPs-MET and Nio-MET are more stable in storage at 4 °C compared to room temperature [40-42].



One of the important features of a novel drug delivery system is the control release capability of drugs at the targeted tissue. In this work, the drug release study of Nio-PEG-MNPs-MET and Nio-MET was evaluated in an SDS-PBS medium with gentle stirring at 37 °C for 72 h. The release rate of MET from Nio-PEG-MNPs-MET and Nio-MET was evaluated at gastric fluid condition (pH = 1.2), pathological cancerous (pH = 5.4) and physiological condition (pH = 7.4). According to Figure 5, the drug releases were independent of pH rate. The most rapid drug release is shown at pH = 1.2, which represents the pH of gastric fluid. A gradual release of the drug is present at pH = 7.4 which represents the pH of the physiological condition. In addition, the drug release at pH = 5.4 was faster, which is one of the necessities for the delivery of anticancer phytochemical drugs like MET to the acidic condition of cancer tissues. The outcomes have proven the major role of Nio in preventing the quick release of drugs at physiological conditions (pH = 7.4). Nio-PEG-MNPs-MET and Nio-MET represented a biphasic release curve with an initial quick release in the

first 8 h. in the following, after quick release, slow releases were observed of 25% and 35% for Nio-PEG-MNPs-MET and Nio-MET formulations, respectively. After the release of drugs within 72 h, there is a fixed phase for all curves. When the pH drops the release of MET increases in 72 h (75 % and 85 % for Nio-PEG-MNPs-MET and Nio-MET, respectively). The main reason for this is the swelling of Nio in acidic conditions and as a result, breaking the Nio. Another reason for this behavior may refer to the quick hydrolysis of surfactants at acidic conditions, causing to release of drugs in lower acidic pH. Since 95% of the free MET was released during the initial 8 h from the dialysis membrane, while the Nio-PEG-MNPs-MET showed a gradual release than free MET and Nio-MET formulation. This feature proves the potential of modified Nio for targeted delivery of MET into the cancerous tissue. Briefly, this drug release test demonstrated that the Nio-PEG-MNPs-MET could make better the availability of the MET for a more extended time. Hence the cytotoxic effects become diminished and the outcomes were completely in agreement with the past studies [43-45].

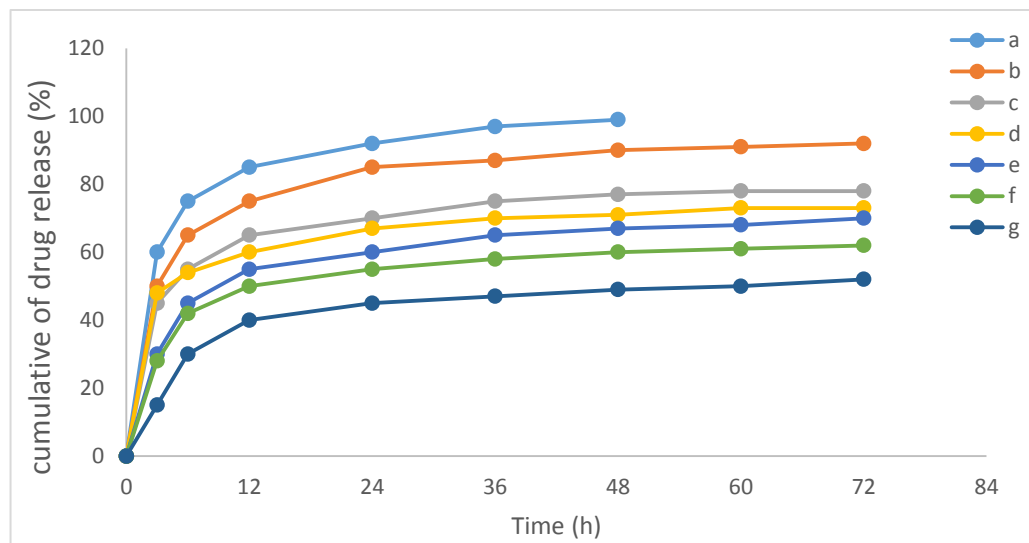


**Figure 5.** In vitro drug release status of MET from the Nio-PEG-MNPs-MET and Nio-MET formulations at 37 °C. (a) Free MET, (b) Nio-MET at pH=1.2, (c) Nio-MET at pH=5.4 (d) Nio-PEG-MNPs-MET at pH=1.2, (e) Nio-PEG-MNPs-MET at pH=5.4, (f) Nio-MET at pH=7.4, (g) Nio-PEG-MNPs-MET at pH=7.4; MET: metformin, Nio: niosome, PEG: Polyethylene Glycol, MNPs: magnetic nanoparticles.

### Cell cytotoxicity of MNPs

The results of this study showed that MET should prevent the expansion of A549 cancer cells. While entrapped MET in various niosomal formulations has efficient synergistic effects in analogy to free form. The encapsulation of MET in PEGylated Nio as well as can overcome the side effects and toxicity and approximately barricade the expansion of the A549 cell line in a dose and time-dependent method. The empty Nio does not have any notable effect on the A549 cell line even in upper doses. Figure 6 demonstrates the effect of the incubation period of MET-loaded-Nio with A549 cell lines on  $IC_{50}$ . according to Figure 6, the amount of  $IC_{50}$  for all 3 samples (free Nio, Nio-MET and Nio-PEG-MNPs-MET) reduced considerably by increasing the period from 24 h to 72 h on A549 cell lines. The amounts of  $IC_{50}$  on A549 cell lines at 48 h were  $12.02 \text{ mM} \pm 1.3\%$ ,  $70 \text{ } \mu\text{g/mL} \pm 1.9\%$  and  $18 \text{ } \mu\text{g/mL} \pm 2.3\%$  for the free MET, Nio-MET and Nio-PEG-MNPs-MET, respectively. The  $IC_{50}$

amounts at 72 h of incubation with A549 cell lines exhibited a similar process for the various drug formulations ( $3.9 \text{ mM} \pm 1.5\%$  (free MET),  $52 \text{ } \mu\text{g/mL} \pm 0.98\%$  (Nio-MET) and  $13 \text{ } \mu\text{g/mL} \pm 1.9\%$  (Nio-PEG-MNPs-MET). Moreover, as demonstrated in Figure 6, the  $IC_{50}$  of the drug-loaded in Nio was considerably decreased compared with the free MET at both drug treatment periods (48 h and 72 h) on A549 cell lines. Also, the Nio-PEG-MNPs-MET demonstrates a notable decrease in  $IC_{50}$  compared with Nio-MET and free MET, proving that a low concentration of MET is efficient, so will have lower cytotoxicity in the patient treatment. Based on the curves shown in Figure 6, the Nio-PEG-MNPs-MET has lower  $IC_{50}$  than free MET and Nio-MET on A549 cell lines. Surveys showed that Nio can efficiently deliver phytochemical drugs to various cancerous cells, and PEGylated-Nio did not cause cytotoxicity [46-49].

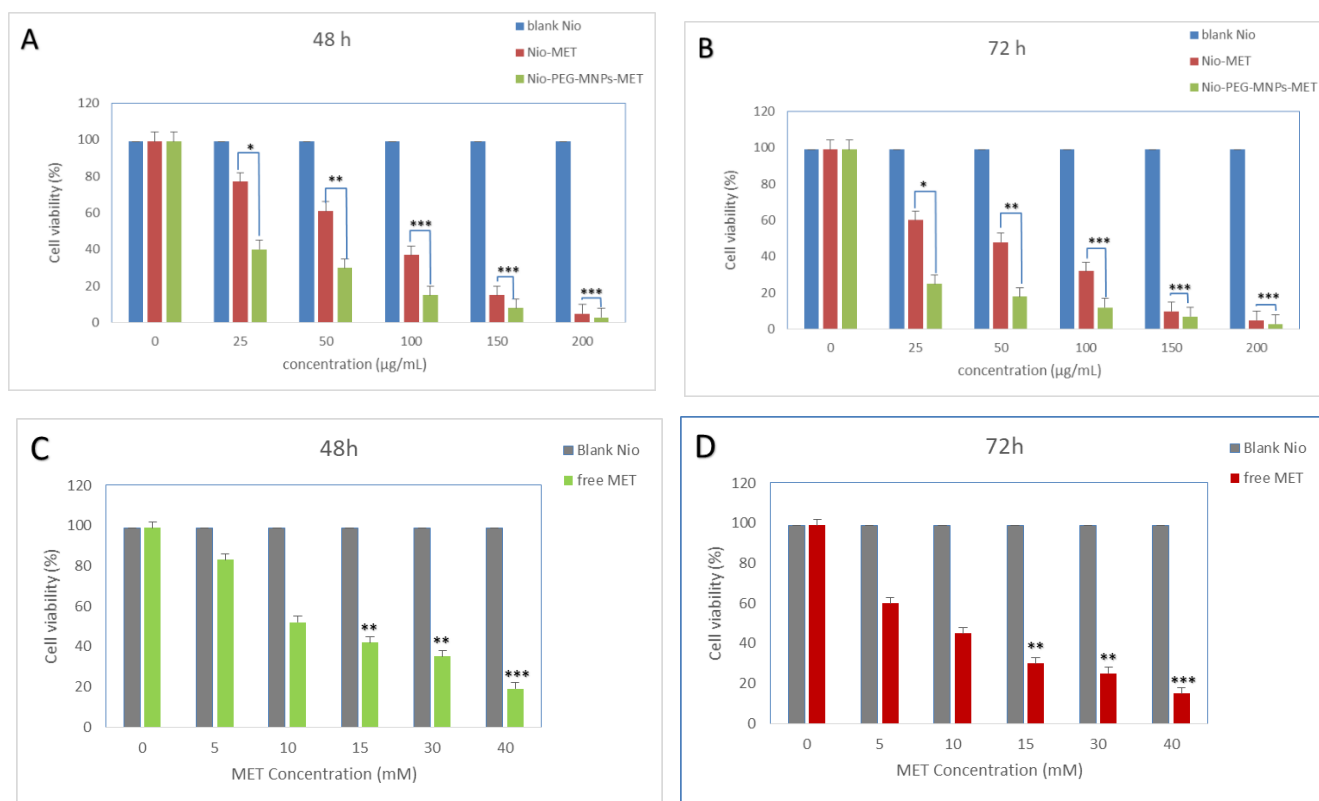


**Figure 6.** *In vitro* cytotoxicity of blank Nio, Nio-MET and Nio-PEG-MNPs-MET against A549 cancer cell lines A) 48 h and B) 72 h. blank Nio and free MET C) 48 h and D) 72 h. Data are represented as Mean  $\pm$  SD from three independent. (\*\*\*:  $p < 0.001$ , \*\*:  $p < 0.01$  and \*:  $p < 0.05$ ); MET: metformin, Nio: niosome, PEG: Polyethylene Glycol, MNPs: magnetic nanoparticles.

## Real-time PCR

for evaluation of the anti-cancer effects of free MET and various niosomal formulations in the A549 cancer cell line, the transcription levels of BCL-2 and BAX genes were investigated by Real-time PCR technique. BCL-2 and BAX (anti-apoptotic and pro-apoptotic, respectively) are dependent on the BCL-2 group, which adjusts the apoptosis procedure via the mitochondrial route. Recent work has demonstrated that the expression of BCL-2 in cancer cells leads to drug resistance, and the expression of BAX in cancerous cells was

related to promising results. As a result, it is estimated that changes in BAX and BCL-2 will lead to apoptosis and barricade the growth of cancerous cells. In this study, it is proven that Nio-PEG-MNPs-MET, Nio-MET and free MET induce the expression level of the BAX gene and prevent the expression of the BCL-2 gene. According to our study results (Figure 7), it is proven that Nio-PEG-MNPs-MET may prevent the viability of lung cancerous cells through the reduction of BCL-2 levels compared to free MET [50-54].

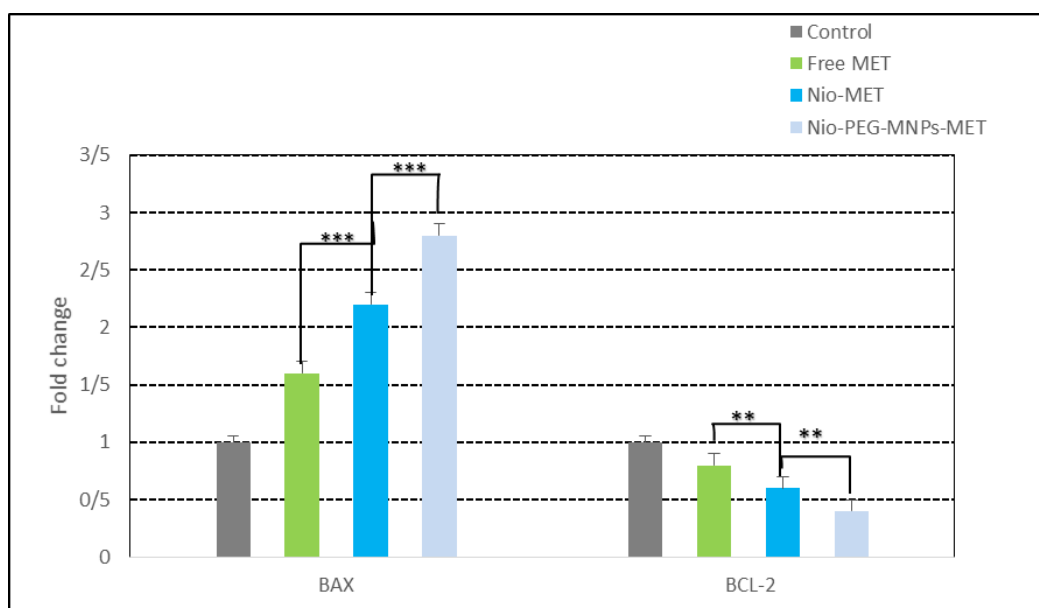


**Figure 7.** The expression of (a) BCL-2 and (b) BAX genes in A549 cell lines after treatment with different formulations. Data are represented as Mean  $\pm$  SD from three independent experiments (\*\*\*)  $p < 0.001$ , \*\*  $p < 0.01$  and \*  $p < 0.05$ ); MET: metformin, Nio: niosome, PEG: Polyethylene Glycol, MNPs: magnetic nanoparticles.

## Conclusion

In this study, Nio-PEG-MNPs-MET was successfully synthesized for the novel targeted drug delivery system to lung cancerous cells. The Nio various formulations were optimized and evaluated in terms of EE%, PDI and size. Also, the release rate of MET was advanced in the pathological cancer condition. According to the results of this study, the acidic pH of cancer tumors generally improves drug release and following that expedites the treatment action. Additionally, the Nio-PEG improves the cytotoxicity against lung cancerous cells. Interestingly, the cell viability state demonstrated that the lung cancerous cells

treatment with Nio-PEG-MNPs-MET represents a notable decrease in terms of the number compared with other samples. The upregulation of the BAX gene and downregulation of the BCL-2 gene expression were increased when lung cancerous cells were treated with the Nio-PEG-MNPs-MET formulation. It can be concluded that the Nio-PEG-MNPs-MET formulation is more efficient even at low dosages. Additionally, the Nio-PEG-MNPs-MET formulation decreases the migration rate of lung cancerous cells, which is necessary for barricading metastasis. In conclusion, we designed and optimized an efficient novel drug delivery system nano-carrier for the targeted therapy of lung

cancerous cells that has minimum side effects on normal cells.

### Acknowledgments

We would like to thank the Tabriz University of Medical Sciences and Islamic Azad University Science and research branch for all their support.

### Data availability statement

All data that prove the findings of this study are accessible on demand from the corresponding authors.

### References

- [1] Ferlay J, Ervik M, Lam F, Colombet M, Mery L, Piñeros M, et al. Global cancer observatory: cancer today. Lyon: International Agency for Research on Cancer; 2020. Cancer Tomorrow. 2021.
- [2] de Groot PM, Wu CC, Carter BW, Munden RF. The epidemiology of lung cancer. *Translational lung cancer research*. **2018**, *7*, 220.
- [3] Gridelli C, Rossi A, Carbone DP, Guarize J, Karachaliou N, Mok T, et al. Non-small-cell lung cancer. *Nature reviews Disease primers*. **2015**, *1*,1-16.
- [4] Urruticoechea A, Alemany R, Balart J, Villanueva A, Vinals F, Capella G. Recent advances in cancer therapy: an overview. *Current pharmaceutical design*. **2010**, *16*, 3-10.
- [5] Mazzotta E, Romeo M, Muzzalupo R. Vesicular drug delivery systems: a novel approach in current nanomedicine. *Molecular Pharmaceutics and Nano Drug Delivery*. **2024**, 135-59.
- [6] Awasthi R, Roseblade A, Hansbro PM, Rathbone MJ, Dua K, Bebawy M. Nanoparticles in cancer treatment: opportunities and obstacles. *Current drug targets*. **2018**, *19*, 1696-709.
- [7] Khan H, Ullah H, Martorell M, Valdes SE, Belwal T, Tejada S, et al., editors. Flavonoids nanoparticles in cancer: Treatment, prevention and clinical prospects. *Seminars in cancer biology*; **2021**: Elsevier.
- [8] Joy C, Nair SK, Kumar KK, Dineshkumar B. Niosomes as nano-carrier based targeted drug delivery system. *Journal of Drug Delivery and Therapeutics*. **2021**,*11*,166-70.
- [9] Mishra V, Nayak P, Singh M, Sriram P, Sutte A. Niosomes: Potential nanocarriers for drug delivery. *J Pharm Clin Res*. **2020**,*11*, 389-94.
- [10] Bajpai S, Tiwary SK, Sonker M, Joshi A, Gupta V, Kumar Y, et al. Recent advances in nanoparticle-based cancer treatment: a review. *ACS Applied Nano Materials*. **2021**, *4*, 6441-70.
- [11] Nowroozi F, Almasi A, Javidi J, Haeri A, Dadashzadeh S. Effect of surfactant type, cholesterol content and various downsizing methods on the particle size of niosomes. *Iranian journal of pharmaceutical Research: IJPR*. **2018**, *17*, 1.
- [12] Maurer V, Altin S, Ag Seleci D, Zarinwall A, Temel B, Vogt PM, et al. In-vitro application of magnetic hybrid niosomes: targeted siRNA-delivery for enhanced breast cancer therapy. *Pharmaceutics*. **2021**,*13*, 394.
- [13] Davarpanah F, Khalili Yazdi A, Barani M, Mirzaei M, Torkzadeh-Mahani M. Magnetic delivery of antitumor carboplatin by using PEGylated-Niosomes. *DARU Journal of Pharmaceutical Sciences*. **2018**, *26*, 57-64.
- [14] d'Avanzo N, Sidorenko V, Simón-Gracia L, Rocchi A, Ottonelli I, Ruozi B, et al. C-end rule peptide-guided niosomes for prostate cancer cell targeting. *Journal of Drug Delivery Science and Technology*. **2024**, *91*, 105162.
- [15] Choudhari AS, Mandave PC, Deshpande M, Ranjekar P, Prakash O. Phytochemicals in cancer treatment: From preclinical studies to clinical practice. *Frontiers in pharmacology*. **2020**,*10*,1614.
- [16] Mallik R, Chowdhury TA. Metformin in cancer. *Diabetes research and clinical practice*. 2018;*143*:409-19.
- [17] Bailey CJ. Metformin: historical overview. *Diabetologia*. **2017**, *60*, 1566-76.
- [18] Lei Y, Yi Y, Liu Y, Liu X, Keller ET, Qian C-N, et al. Metformin targets multiple signaling pathways in cancer. *Chinese journal of cancer*. **2017**, *36*,1-9.
- [19] Sacco F, Calderone A, Castagnoli L, Cesareni G. The cell-autonomous mechanisms underlying the activity of metformin as an anticancer drug. *British Journal of Cancer*. **2016**, *115*,1451-6.
- [20] Kenekwue FC, Nnamani DO, Duhu JC, Nmesirionye BU, Momoh MA, Akpa PA, et al. Potential enhancement of metformin hydrochloride in solidified reverse micellar solution-based PEGylated lipid nanoparticles targeting therapeutic efficacy in diabetes treatment. *Heliyon*. **2022**, *8*.
- [21] Zhang Q, Hu N. Effects of metformin on the gut microbiota in obesity and type 2 diabetes mellitus. *Diabetes, Metabolic Syndrome and Obesity*. **2020**, 5003-14.
- [22] Ebrahimnezhad Z, Zarghami N, Keyhani M, Amirsaadat S, Akbarzadeh A, Rahmati M, et al. Inhibition of hTERT gene expression by silibinin-loaded PLGA-PEG-Fe<sub>3</sub>O<sub>4</sub> in T47D breast cancer cell line. *BioImpacts: BI*. **2013**, *3*, 67.
- [23] Ma B, Li Q, Mi Y, Zhang J, Tan W, Guo Z. pH-responsive nanogels with enhanced antioxidant and antitumor activities on drug delivery and smart drug release. *International Journal of Biological Macromolecules*. **2024**, *257*,128590.
- [24] Haynes S. Side Effects of Metformin (Glucophage, Formamet, Glumetza). *Digestion*. **2024**.

- [25] Mogheri F, Jokar E, Afshin R, Akbari AA, Dadashpour M, Firouzi-amandi A, et al. Co-delivery of metformin and silibinin in dual-drug loaded nanoparticles synergistically improves chemotherapy in human non-small cell lung cancer A549 cells. *Journal of Drug Delivery Science and Technology*. **2021**, 66,102752.
- [26] Elumalai K, Srinivasan S, Shanmugam A. Review of the efficacy of nanoparticle-based drug delivery systems for cancer treatment. *Biomedical Technology*. **2024**, 5, 109-22.
- [27] El-Ridy MS, Yehia SA, Elsayed I, Younis MM, Abdel-Rahman RF, El-Gamil MA. Metformin hydrochloride and wound healing: from nanoformulation to pharmacological evaluation. *Journal of liposome research*. **2019**, 29, 343-56.
- [28] Akbarzadeh I, Keramati M, Azadi A, Afzali E, Shahbazi R, Norouzian D, et al. Optimization, physicochemical characterization, and antimicrobial activity of a novel simvastatin nano-niosomal gel against *E. coli* and *S. aureus*. *Chemistry and Physics of Lipids*. **2021**, 234,105019.
- [29] Thabet Y, Elsabahy M, Eissa NG. Methods for preparation of niosomes: A focus on thin-film hydration method. *Methods*. **2022**, 199, 9-15.
- [30] Ghafelehbashir R, Akbarzadeh I, Yarak MT, Lajevardi A, Fatemizadeh M, Saremi LH. Preparation, physicochemical properties, in vitro evaluation and release behavior of cephalixin-loaded niosomes. *International journal of pharmaceutics*. **2019**, 569,118580.
- [31] Javidfar S, Pilehvar-Soltanahmadi Y, Farajzadeh R, Lotfi-Attari J, Shafiei-Irannejad V, Hashemi M, et al. The inhibitory effects of nano-encapsulated metformin on growth and hTERT expression in breast cancer cells. *Journal of drug delivery science and technology*. **2018**, 43, 19-26.
- [32] Shahbazi R, Babazadeh M, Afzali E. Surface modification of silica-coated on the magnetic nanoparticles with covalently immobilized between imidazolium cation and silane groups for potential application as a green catalyst. *MOJ Biorg Org Chem*. **2018**, 2, 11-7.
- [33] Shahbazi R, Jafari-Gharabaghloou D, Mirjafary Z, Saeidian H, Zarghami N. Design and optimization various formulations of PEGylated niosomal nanoparticles loaded with phytochemical agents: potential anti-cancer effects against human lung cancer cells. *Pharmacological Reports*. **2023**, 75, 442-55.
- [34] Nisha R, Kumar P, Gautam AK, Bera H, Bhattacharya B, Parashar P, et al. Assessments of in vitro and in vivo antineoplastic potentials of  $\beta$ -sitosterol-loaded PEGylated niosomes against hepatocellular carcinoma. *Journal of Liposome Research*. **2020**, 31, 304-15.
- [35] Amiri B, Ebrahimi-Far M, Saffari Z, Akbarzadeh A, Soleimani E, Chiani M. Preparation, characterization and cytotoxicity of silibinin-containing nanoniosomes in T47D human breast carcinoma cells. *Asian Pacific Journal of Cancer Prevention*. **2016**, 17, 3835-8.
- [36] Hasan AA, Madkor H, Wageh S. Formulation and evaluation of metformin hydrochloride-loaded niosomes as controlled release drug delivery system. *Drug delivery*. **2013**, 20,120-6.
- [37] Mohamad Saimi NI, Salim N, Ahmad N, Abdulmalek E, Abdul Rahman MB. Aerosolized niosome formulation containing gemcitabine and cisplatin for lung cancer treatment: Optimization, characterization and in vitro evaluation. *Pharmaceutics*. **2021**, 13, 59.
- [38] Morelli AP, Tortelli Jr TC, Pavan ICB, Silva FR, Granato DC, Peruca GF, et al. Metformin impairs cisplatin resistance effects in A549 lung cancer cells through mTOR signaling and other metabolic pathways. *International journal of oncology*. **2021**, 58, 1-15.
- [39] Balasubramaniam A, Anil Kumar V, Sadasivan Pillai K. Formulation and in vivo evaluation of niosome-encapsulated daunorubicin hydrochloride. *Drug development and industrial pharmacy*. **2002**, 28,1181-93.
- [40] Akbarzadeh I, Saremi Poor A, Yaghmaei S, Norouzian D, Noorbazargan H, Saffar S, et al. Niosomal delivery of simvastatin to MDA-MB-231 cancer cells. *Drug Development and Industrial Pharmacy*. **2020**, 46, 1535-49.
- [41] Pilehvar-Soltanahmadi Y, Nouri M, Martino MM, Fattahi A, Alizadeh E, Darabi M, et al. Cytoprotection, proliferation and epidermal differentiation of adipose tissue-derived stem cells on emu oil based electrospun nanofibrous mat. *Experimental cell research*. **2017**, 357, 192-201.
- [42] Li B, Takeda T, Tsuiji K, Kondo A, Kitamura M, Wong TF, et al. The antidiabetic drug metformin inhibits uterine leiomyoma cell proliferation via an AMP-activated protein kinase signaling pathway. *Gynecological Endocrinology*. **2013**, 29, 87-90.
- [43] Eskandari Z, Bahadori F, Celik B, Onyuksel H. Targeted nanomedicines for cancer therapy, from basics to clinical trials. *Journal of Pharmacy & Pharmaceutical Sciences*. **2020**, 23, 132-57.
- [44] Dash S, Murthy PN, Nath L, Chowdhury P. Kinetic modeling on drug release from controlled drug delivery systems. *Acta Pol Pharm*. **2010**, 67, 217-23.
- [45] Naderinezhad S, Amoabediny G, Haghirsadat F. Co-delivery of hydrophilic and hydrophobic anticancer drugs using biocompatible pH-sensitive lipid-based nano-carriers for multidrug-resistant cancers. *RSC advances*. **2017**, 7, 30008-19.
- [46] Storozhuk Y, Hopmans S, Sanli T, Barron C, Tsiani E, Cutz J, et al. Metformin inhibits growth and enhances radiation response of non-small cell lung cancer

(NSCLC) through ATM and AMPK. *British journal of cancer*. **2013**, 108, 2021-32.

[47] Wang Y, Lin B, Wu J, Zhang H, Wu B. Metformin inhibits the proliferation of A549/CDDP cells by activating p38 mitogen-activated protein kinase. *Oncology letters*. **2014**, 8, 1269-74.

[48] Dong X-L, Yang E, Sun B-N, Liu Y-Q, Zhou J. Antineoplastic activity of metformin on the A549 human lung carcinoma cell line in vitro. *Int J Clin Exp Med*. **2017**, 10, 10711-7.

[49] Ashinuma H, Takiguchi Y, Kitazono S, Kitazono-Saitoh M, Kitamura A, Chiba T, et al. Antiproliferative action of metformin in human lung cancer cell lines. *Oncology reports*. **2012**, 28, 8-14.

[50] Li H, Qiu Z, Li F, Wang C. The relationship between MMP-2 and MMP-9 expression levels with

breast cancer incidence and prognosis. *Oncology letters*. **2017**, 14, 5865-70.

[51] Lanshan Huang M, Fanghui Ren M, Ruixue Tang M. Prognostic Value of Expression of Cyclin E in Gastrointestinal Cancer: A Systematic Review and Meta-Analysis. **2015**.

[52].Boice A, Bouchier-Hayes L. Targeting apoptotic caspases in cancer. *Biochimica et Biophysica Acta (BBA)-Molecular Cell Research*. **2020**, 1867,118688.

[53] Pfeffer CM, Singh AT. Apoptosis: a target for anticancer therapy. *International journal of molecular sciences*. **2018**, 19, 448.

[54] Li J, Yuan J. Caspases in apoptosis and beyond. *Oncogene*. **2008**, 27, 6194-206.